The Thesis Committee for Dongyang Chen
Certifies that this is the approved version of the following thesis:

Experimental Characterization of Bowden Cable Friction and Compliance

APPROVED BY
SUPERVISING COMMITTEE:

Supervisor:

Ashish Deshpande

Luis Sentis

Experimental Characterization of Bowden Cable Friction and Compliance

by

Dongyang Chen, B.S.

THESIS

Presented to the Faculty of the Graduate School of

The University of Texas at Austin

in Partial Fulfillment

of the Requirements

for the Degree of

MASTER OF SCIENCE IN ENGINEERING

THE UNIVERSITY OF TEXAS AT AUSTIN

August 2014

Dedicated to my family, girlfriend and friends.

Acknowledgments

I would like to thank numerous people who made this thesis possible.

Foremost, I would like to express my sincere gratitude to my research advisor, Dr. Ashish D. Deshpande, for his endless support and guidance. He has always instructed me to carry out structured research to interpret results. Many ideas are inspired from our in depth discussions. Moreover, his strict and methodical approach to research has influenced me profoundly and will stick with me doing my future endeavors. I would also like to thank Dr. Luis Sentis for serving as my committee member and offering precious advices.

Next, I would like to acknowledge my fellow lab members, Youngmok Yun and Priyanshu Agarwal, who have been a invaluable resources. Also, I am grateful for the help from Prashant Rao, Jonas Fox, and all the other members in our lab.

Finally, I would like to thank my family members, especially my parents, for their love, patience and support. Without them I can not imagine the person I would be today. Lastly, I am grateful to my family and friends who make me feel like I can do anything.

Experimental Characterization of Bowden Cable Friction and Compliance

Dongyang Chen, M.S.E.
The University of Texas at Austin, 2014

Supervisor: Ashish D. Deshpande

This thesis presents a systematic method for experimental characterization of Bowden cable friction and compliance. A novel tension and elongation measurement method using a motion capture system and a spring is introduced. With the measurement method, the effects of nine variables on friction and cable compliance are investigated through a comprehensive set of experiments under 144 different cases. We have generated specific guidelines for Bowden cable configurations and design parameters to achieve optimal performance which may help robotics researchers in choosing and configuring Bowden cables, and designing control systems for actuation.

Table of Contents

Acknowledgments **v**

Abstract **vi**

List of Figures **iii**

Chapter 1. Introduction **1**

Chapter 2. Existing Mathematical Models **6**

Chapter 3. Experiment Design **10**

3.1 Factors Selection 10

3.1.1 Cable Construction 11

3.1.2 Cable Diameter 11

3.1.3 Sheath Thickness 12

3.1.4 Cable and Sheath Material 12

3.1.5 Bending Angle 13

3.1.6 Pretension 13

3.1.7 Cable Speed 13

3.1.8 Sheath Routing 14

3.2 Evaluation Criteria 17

3.3 Measurement Method 19

3.3.1 Tension Measurement 19

3.3.2 Elongation Measurement 20

3.4 Experimental Setup 20

3.5 Experiment Procedure 21

3.5.1 For Friction Characterization Experiments 22

3.5.2 For Compliance Characterization Experiments 24

Chapter 4. Experimental Results **25**
4.1 Friction Characterization 25
4.1.1 Cable Construction (Fig. 4.1) 25
4.1.2 Cable Diameter (Fig. 4.2) 26
4.1.3 Sheath Thickness (Fig. 4.3) 27
4.1.4 Cable (Fig. 4.4) and Sheath Material (Fig. 4.5) 27
4.1.5 Bending Angle (Fig. 4.7) 30
4.1.6 Pretension (Fig. 4.8) 33
4.1.7 Cable Speed (Fig. 4.9) 33
4.1.8 Sheath Routing (Fig. 4.1–4.9) 33
4.2 Compliance Characterization 34
4.2.1 Cable Construction (Fig. 4.10) 34
4.2.2 Cable Diameter (Fig. 4.11) 34
4.2.3 Sheath Thickness (Fig. 4.12) 35
4.2.4 Cable and Sheath Material 36
4.2.5 Bending Angle (Fig. 4.14) 37
4.2.6 Pretension (Fig. 4.15) 37
4.2.7 Cable Speed (Fig. 4.16) 39
4.2.8 Sheath Routing (Fig. 4.10–4.16) 39

Chapter 5. Conclusions **41**

Appendix **45**

Appendix 1. Data **46**

Bibliography **51**

List of Figures

1.1 **Typical input-output curve for comparison between experimental and simulation results (7x19 stainless steel cable, PTFE sheath, 90° angle, 500 mm cable length).** 5

2.1 **Force balance for an infinitesimal tendon element.** . . . 7

3.1 **Cable construction types.** 11
3.2 **Cables and sheaths analyzed in our experiments.** . . . 16
3.3 **Validation of the new force measurement method.** . . . 18
3.4 **Experimental setups.** 21
3.5 **Typical plots of experiment trials** 22

4.1 **Effects of cable construction on force transmission efficiency (PTFE thin sheath, 90° bending angle, $4N$ pretension, $0.0153\ m/s$ cable speed).** 26
4.2 **Effects of cable diameter on force transmission efficiency (PTFE thin sheath, 90° bending angle, $4N$ pretension, $0.0153\ m/s$ cable speed).** 27
4.3 **Effects of sheath thickness on force transmission efficiency (7x19 FEP-coated large-diameter cable, 90° bending angle, $4N$ pretension, $0.0153\ m/s$ cable speed).** . . . 28
4.4 **Effects of cable material on force transmission efficiency (Nylon sheath, 90° bending angle, $4N$ pretension, $0.0153\ m/s$ cable speed).** 29
4.5 **Effects of sheath material on force transmission efficiency (7x19 stainless steel cable, 90° bending angle, $4N$ pretension, $0.0153\ m/s$ cable speed).** 30
4.6 **Effects of cable material on force transmission efficiency (PTFE thin sheath, 90° bending angle, $4N$ pretension, $0.0153\ m/s$ cable speed).** 31
4.7 **Effects of bending angle on force transmission efficiency (PTFE thin sheath, 1x7 stainless steel cable, $4N$ pretension, $0.0153\ m/s$ cable speed).** 31

4.8 **Effects of pretension on force transmission efficiency (PTFE thin sheath, 90° bending angle, 7x19 stainless steel cable, $0.0153\ m/s$ cable speed).** 32

4.9 **Effects of speed on force transmission efficiency (PTFE thin sheath, 90° bending angle, $4N$ pretension, 1x7 stainless steel cable).** 32

4.10 **Effects of cable construction on elongation compliance (PTFE thin sheath, 90° bending angle, $4N$ pretension, $0.0153\ m/s$ cable speed).** 34

4.11 **Effects of cable diameter on elongation compliance (PTFE thin sheath, 90° bending angle, $4N$ pretension, $0.0153\ m/s$ cable speed).** 35

4.12 **Effects of sheath thickness on elongation compliance (7x19 FEP-coated large-diameter cable, 90° bending angle, $4N$ pretension, $0.0153\ m/s$ cable speed).** 36

4.13 **Effects of sheath thickness on force transmission efficiency (7x19 FEP-coated large-diameter cable, 90° bending angle, $4N$ pretension, $0.0153\ m/s$ cable speed, with pulley).** 37

4.14 **Effects of bending angle elongation compliance (PTFE thin sheath, 1x7 stainless steel cable, $4N$ pretension, $0.0153\ m/s$ cable speed).** 38

4.15 **Effects of pretension on elongation compliance (PTFE thin sheath, 90° bending angle, 7x19 stainless steel cable, $0.0153\ m/s$ cable speed).** 38

4.16 **Effects of speed on elongation compliance (PTFE thin sheath, 90° bending angle, $4N$ pretension, 1x7 stainless steel cable).** 39

Chapter 1

Introduction

A Bowden cable is a type of flexible cable used to transmit mechanical force or motion by the movement of an inner cable relative to a hollow outer sheath. It is commonly used on bike and vehicle break systems. Recently, many robotic researchers, particularly those who design wearable robots and medical devices, have introduced Bowden cables into robot applications [3, 4, 19, 20, 22, 23, 26, 27]. We also plan to use Bowden cable actuation in a novel hand exoskeleton [1].

Bowden cables have several advantages which make them suitable for robotics applications. The first one is remote actuation. Many robot systems suffer adversely from the mass and moment of inertia of actuators and transmission systems because they affect the dynamic properties of the system. The mass and moment of inertia especially degrade the dynamic transparency of wearable robots. By using a Bowden cable, actuators can be placed far away from end-effectors, which helps to reduce the weight and inertia and increase the power density. The second advantage is flexibility. Most mechanical transmission systems such as gear trains, belts and tendon-pulleys are rigid and the configuration of the system is fixed. However, since the only interaction be-

tween a Bowden cable and other systems or environment is at its two ends where they are clamped, it is flexible and free to move in between and this helps to increase the range of motion of end-effectors. Third, a Bowden cable is only clamped at the ends and no support is needed to change its routing path, which means the location where reaction forces are exerted by other parts or environment on the end-effector can be changed by using Bowden cables and this helps to decouple the actuated end-effector.

However, the critical weakness of a Bowden cable is its nonlinear characteristics due to cable and sheath compliance and the friction between its inner cable and outer sheath. These characteristics degrade the performance of the transmission system. [14] report that up to 95% of the motor torque is used to overcome Bowden cable friction. And [9] report that the stability of their force servo system depends on input due to such nonlinear characteristics. Despite the significant influence of the friction and compliance, many robotics researchers have neglected them in their system models and treated them as disturbances in the control schemes [23][13][21]. The primary reason for this is that it is difficult to model and compensate for them due to their non-linearity and multi-variable dependency.

The nonlinear and multi-variable dependent characteristics of Bowden cable is a result of the nature of friction, and modeling friction is a key part of Bowden cable frictions. Kaneko et al. [11][10] first introduced a static model incorporating both tendon compliance and Coulomb friction. They also proposed a lumped parameters dynamic model for numerical simulation. Palli

et al. [17] and Chen et al. [15] modified these models by using Dahl model and Lugre model which can better reflect various friction behaviors, such as presliding displacement and Stribeck effect. Wang et al. [25] extended two-dimensional results to simple three-dimensional Bowden cable configuration. Agrawal et al. [2] proposed a mathematically rigorous distributed parameter model for configurations with any curvature and initial tension profile.

However, the performance of Bowden cable is still difficult to predict with the above models. There are several reasons for that. First, Bowden cable behavior depends on many variables including material properties, configuration, working load etc, which may not be counted in these models. Second, these models[10, 11, 17] use assumptions that are not applicable under real situations, such as constant wrapping angles and uniform pretension along the sheath. Third, the initial conditions are hard to determine when simulating any dynamic models proposed in the studies above. Finally, simple friction models can not account for all the friction behaviors while complex friction models have many coefficients which are not easy to determine. Even though the values of these parameters can be estimated through system identification, these models can not accurately predict the behavior of Bowden cables once the working condition is not the same as the condition under which the system identification is carried out, as shown in Fig. 1.1. We collected experimental data with 1 Hz sinusoidal input and 4 N pretension and used these data to identify the coefficients in Dahl model. Fig. 1.1(a) shows that the simulated curve using the identified coeffeicients is very close to the real experimental

curve. However, the simulated curve deviates from the experimental curve when the input frequency and pretension are changed to 5 Hz and 6 N respectively.

Given the critical challenges in modeling Bowden cable transmission, we decide to characterize Bowden cable performance and gain an understanding of effects of design parameters by conducting extensive experiments. The design of experiments is based on the knowledge gained from study of existing models. Only limited experimental studies have been carried out with Bowden cables. Goiriena et al. [8] only partially showed the influence of some variables on friction using only steel cables and one sheath. There is no systematic method for characterizing the performance of Bowden cables, leading to a difficulty in the selection of proper Bowden cables and in designing control systems for Bowden cable actuated robots.

This theis presents a systematic experimental method for the characterization of small-sized Bowden cable systems used either for force or motion transmission. The theis first introduces the existing mathematical models of Bowden cable and the limitations of current work. Next, the experiment methodology is presented, including factors selection, the performance evaluation criteria, a novel cable tension and elongation measurement technique using a motion capture system and springs, experimental setup and experiment procedure. Finally, the experimental results are shown and discussed about. Initial work on this topic was published in [6].

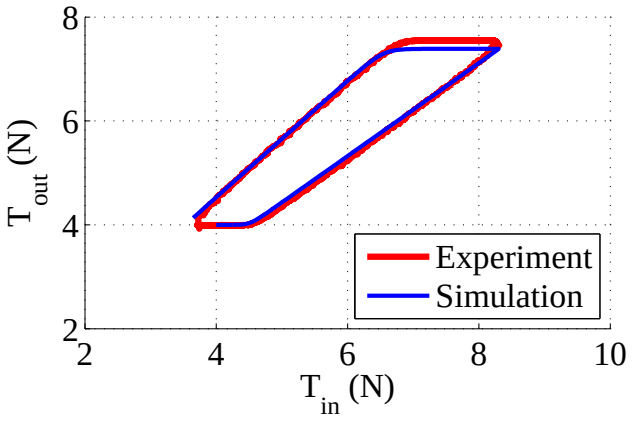

(a) $1Hz$ input, $4N$ pretension

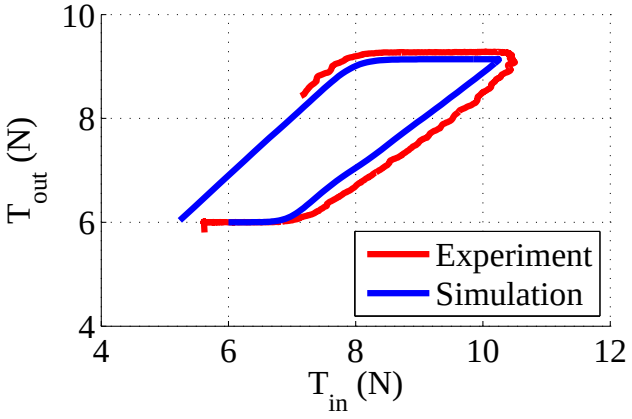

(b) $5Hz$ input, $6N$ pretension

Figure 1.1: **Typical input-output curve for comparison between experimental and simulation results (7x19 stainless steel cable, PTFE sheath,** 90° **angle, 500 mm cable length).** (a) 1 Hz sinusoidal input and 4 N pretension is applied and the experimental data is used to identify the coefficients in Dahl model. (b) 5 Hz sinusoidal input and 6 N pretension is applied and the experimental data is plotted against the data predicted by simulation with the identified parameters.

Chapter 2

Existing Mathematical Models

The static model of a Bowden cable system presented in [11][10] (Fig. 2.1) is:

$$
\begin{aligned}
N &= T(x)d\alpha(x) = T(x)\frac{dx}{r(x)} && (2.1)\\
f &= \mu N sign(\dot{x}) = -dT(x) && (2.2)\\
\mu &= \begin{cases} \mu_s & \text{if } \dot{x} = 0 \\ \mu_d & \text{if } \dot{x} \neq 0 \end{cases} && (2.3)\\
d\delta(x) &= \frac{T(x)}{EA}dx && (2.4)
\end{aligned}
$$

where f, N and $T(x)$ are the friction force, normal force and cable tension, dx and $r(x)$ are the arc length and curvature radius of the cable element, $\alpha(x)$ is the angle enclosed by dx, μ_s and μ_d are the static and dynamic Coulomb friction coefficients, E, A and $\delta(x)$ are the Youngs Modulus, cross section area and elongation of the element. From these equations, we can obtain:

$$
\begin{bmatrix} \frac{dT(x)}{dx} \\ \\ \frac{d\delta(x)}{dx} \end{bmatrix} = \begin{bmatrix} -\frac{\mu}{r(x)}sign(\dot{x}) & 0 \\ \\ \frac{1}{EA} & 0 \end{bmatrix} \begin{bmatrix} T(x) \\ \\ \delta(x) \end{bmatrix} - \begin{bmatrix} 0 \\ \\ -\frac{1}{EA} \end{bmatrix} T_0 \qquad (2.5)
$$

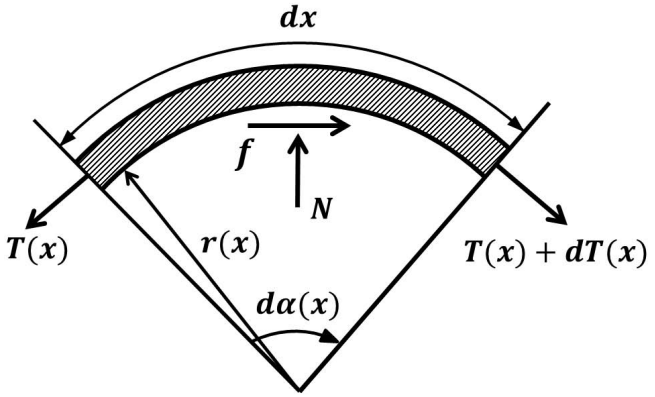

Figure 2.1: **Force balance for an infinitesimal tendon element [15].**

If we assume constant radius R and pretension T_0 along the whole cable length, the analytical solution of the system is:

$$T(x) = \begin{cases} T_{in} exp\left[-\frac{\mu}{R} x sign(\dot{x})\right] & \text{if } x < L_1 \\ T_0 & \text{if } x \geq L_1 \end{cases} \tag{2.6}$$

$$\delta(x) = \begin{cases} \frac{1}{EA}\left[H(x) - T_0 x + \frac{R}{\mu} T_{in} sign(\dot{x})\right] & \text{if } x < L_1 \\ \frac{1}{EA}\left[H(L_1) - T_0 L_1 + \frac{R}{\mu} T_{in} sign(\dot{x})\right] & \text{if } x \geq L_1 \end{cases} \tag{2.7}$$

where

$$H(x) = -\frac{R}{\mu} T_{in} sign(\dot{x}) exp\left[-\frac{\mu}{R} x sign(\dot{x})\right] \tag{2.8}$$

$$L_1 = min\left\{x \in T(x) = T_0\right\} \tag{2.9}$$

L_1 is the maximum length along the cable where the input tension can be transmitted.

Although the solution is simple and helps us in understanding the fundamental characteristics of Bowden cables, it is not applicable for general situations because it is based on some simplified assumptions, such as constant curvature radius and pretension along the whole cable length. In practice, the initial tension profile depends on the time history of past applied forces and is usually not uniform. And due to the flexibility characteristics of a Bowden cable, the curvature radius of the sheath can vary during the operation of the Bowden cable. Therefore, to get the analytical solution, we have to integrate (2.5) along the cable length with varying radius and non-uniform pretension profile. However, it is almost impossible to know the time-variant radius of each infinitesimal cable segment and the pretension profile as well. To numerically solve the problem, Kaneko et al. [11][10] also proposed a lumped parameters model based on Coulomb friction for simulation, which was later refined by using Dahl model [17] and Lugre model [15] which can better reflect various friction behaviours. But they made the same assumptions of constant radius and pretension profile which greatly limit their usefulness in real applications.

There are other limitations of these models. For example, they do not take buckling effect into account. While the cable is under tension, the sheath is under compression due to the interaction between the cable and sheath. When the compression force is large enough, it will cause the sheath to locally buckle and twist, which greatly degrade the force or motion transmission performance. In addition, the coefficients of these models are not necessar-

ily constant, but time or configuration dependent. This makes it even more difficult to accurately model Bowden cables. Actually, numerous factors affect the performance of a Bowden cable. Given the complexity of Bowden cable behaviour, we propose to characterize Bowden cable friction and compliance through experiments. Our goal is to generate guidelines of choosing and configuring Bowden cables.

Chapter 3

Experiment Design

3.1 Factors Selection

Numerous factors affect the performance of a Bowden cable and it is impossible to study all of them, so we have to choose key factors to be investigated. Because our goal is to generate guidelines for choosing and configuring Bowden cables, we decided to select the factors needed to be considered during the process of building a Bowden cable transmission system, of which the first crucial step is to choose the right type of cable and sheath. And the next step is to configure and determine the way of using the Bowden cable. Considering these two steps, we decided to choose the following nine variables for our study: cable construction, cable diameter, cable material, sheath thickness, sheath material, bending angle, pretension, cable speed and sheath routing. And for each one of the nine factors, we used two different values to determine the effects of the factors on the performance of a Bowden cable. We did not include cable length as one of the factors because it is typically decided by specific application situation. For consistency, the cable length is kept as $500mm$ for all situations.

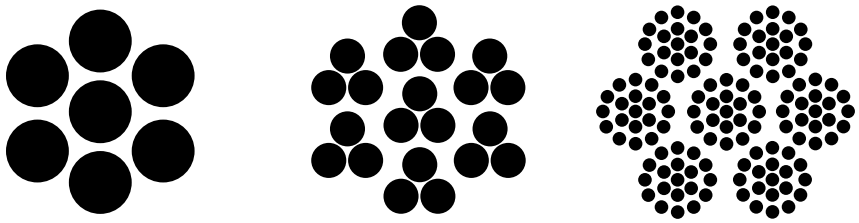

(a) 1x7 (b) 7x3 (c) 7x19

Figure 3.1: **Cable construction types.** The name of a cable indicates its construction, for example an 1x7 cable consists of one strand, each made with seven wires. The construction mainly determines the bending and elongation stiffness of a cable. The 1x7 cables have the largest stiffness, while the 7x19 cables have the smallest stiffness of the same size.

3.1.1 Cable Construction

The construction of a cable means the number of its strands and wires per strand (Fig. 3.1), which is usually indicated by the cable name. For example, a 7x19 cable consists of seven strand, each made with nineteen wires. Cable construction mainly determines the bending stiffness of a cable given the same diameter and material. For the cables we use, 1x7 cables are stiffer than 7x19 cables for bending. Also cable construction will affect the elongation stiffness of a cable. Similarly, 1x7 cables are stiffer than 7x19 cables for elongation.

3.1.2 Cable Diameter

Generally the diameter of cables and sheaths is restricted by the application requirement such as load or space limit. In our experiments, we mainly focus on small-sized Bowden cables since for hand exoskeletons, load require-

ments are relatively small compared with those exoskeletons used for upper or lower limbs. Cable diameter determines its cross section area and thus has effect on both bending stiffness and elongation stiffness. Larger diameter leads to larger bending stiffness and larger elongation stiffness. The two diameters we use for the cables are 0.53 mm and 0.66 mm. And for consistency, the sheath inner diameter is kept as 1 mm.

3.1.3 Sheath Thickness

Given the same inner diameter and material, the bending stiffness of a sheath is mainly determined by its thickness – the thicker the sheaths are, the more difficult it is to bend them and thus they have larger stiffness. Also sheath thickness will affect the elongation stiffness of a sheath. Since thicker sheath has larger cross section area, it also has larger elongation stiffness. The two thickness we use for the sheaths are 0.4 mm and 1.0 mm.

3.1.4 Cable and Sheath Material

There are various materials for cables and sheaths. The major effect of different materials on Bowden cables is their coefficients of friction. We select two types of cables of different materials – stainless steel cable and Fluorinated ethylene propylene (FEP)-coated cable; and two types of sheaths of different materials – Nylon sheath and Polytetrafluoroethene (PTFE) sheath.

3.1.5 Bending Angle

As shown in Fig. 2.1, the bending angle formed by the cable will affect the normal force and in turn change the friction force and elongation. However, it is very difficult to know the exact angles along the whole length of a flexible Bowden cable. Therefore, we use the angle formed by the two sheath clamps instead, which can be quantified easily (θ in Fig. 3.4). The two angles we use for θ are 45° and 90°.

3.1.6 Pretension

Another important factor in setting up Bowden cables is pretension. Because Bowden cables can only work under tension, insufficient pretension would lead to cable slack. On the other hand, excessive pretension will increase the power consumption of the actuator and may also affect the friction and elongation performance of Bowden cables (see (2.5)). However, as stated before, it is impossible to know the exact pretension profile because the profile is not uniform and it depends on the time history of past applied forces. So we only control and change the pretension at the output side of a Bowden cable. The two pretensions we use are 4 N and 6 N.

3.1.7 Cable Speed

According to 2.5, it seems that the magnitude of cable moving speed has no effect on either the friction or the elongation of a Bowden cable. However, in order to control cable movement, especially for position control, the cable

moving speed is an indispensable aspect needed to be considered for Bowden cable application. Therefore, we include it as one of the factors. From (2.6) (2.7), we can see that not all parts of a Bowden cable will always move at the same time. Instead, there might be some portion of a Bowden cable which is moving while the rest is at rest. This makes it very difficult to know the velocity profile along the whole length of a Bowden cable. Thus we only control and change the cable moving speed at the input side of a Bowden cable. The two cable speeds we use are 0.0153 m/s and 0.046 m/s.

3.1.8 Sheath Routing

Due to the interaction between the cable and sheath, the sheath is under compression while the cable is under tension. Moreover, there is no support for the sheath except the two clamps at its two ends. All these facts lead to the movement and even buckling of the sheath, which will greatly affect both the force and motion transmission performance of a Bowden cable. To eliminate this uncertain factor, other researchers [10, 11, 15, 17] route the sheaths around pulleys. But this might not be possible in Bowden cable applications due to space limitation. To get a true understanding of Bowden cable, we decide to carry out experiments under two conditions – one with the sheath routed around a pulley and the other without.

Table 3.1 shows all the nine factors and the two different values for each factor used in our experiments. In summary, we used four types of cables for our experiment (Fig. 3.2), 1x7 stainless steel cable, 7x19 stainless steel cable,

Table 3.1: **Factors selected for the experiments.** There are nine factors in total, including cable construction, cable diameter, cable material, sheath thickness, sheath material, bending angle, pretension, cable speed and sheath routing. Two different values used for each factor are shown in the table.

Cable	**Construction**	1x7/ 7x19
	Diameter (mm)	0.53/ 0.66
	Material	Stainless steel/ FEP-coated
Sheath	**Thickness (mm)**	0.4/ 1.0
	Material	Nylon/ PTFE
Bending angle		45°/ 90°
Pretension (N)		4.0/ 6.0
Cable speed (m/s)		0.0153/ 0.046
Sheath routing		With pulley/ Without pulley

7x19 FEP-coated small-diameter cable and 7x19 FEP-coated large-diameter cable. Except the 7x19 FEP-coated small-diameter cable having a diameter of 0.53 mm, the other three cables share the same diameter of 0.66 mm. Therefore by comparing the experimental results of 1x7 stainless steel cable and 7x19 stainless steel cable, the effect of cable construction can be seen; by comparing the results of 7x19 stainless steel cable and 7x19 FEP-coated large-diameter cable, the effect of cable material can be determined; and by comparing the results of FEP-coated small-diameter and large-diameter cable, the effect of cable diameter can be understood.

We used three types of sheaths for our experiment (Fig. 3.2), PTFE thin sheath, Nylon sheath and PTFE thick sheath. All the three types of sheaths

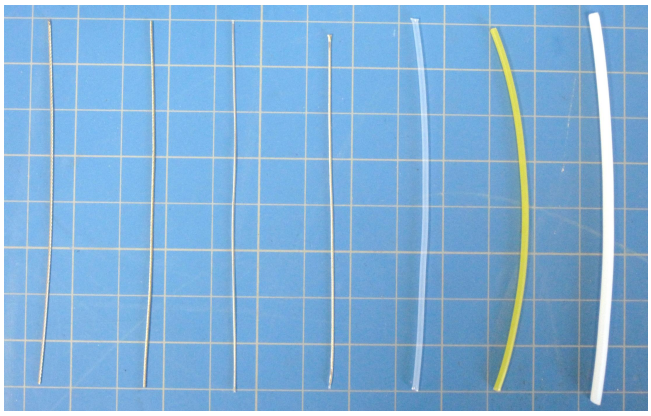

Figure 3.2: **Cables and sheaths analyzed in our experiments.** (a) 1x7 stainless steel cable, (b) 7x19 stainless steel cabl,; (c) 7x19 FEP-coated small-diameter cable, (d) 7x19 FEP-coated large-diameter cable, (e) PTFE thin sheath, (f) Nylon sheath and (g) PTFE thick sheath

share the same inner diameter of 1 mm. The Nylon and PTFE thin sheath also have the same thickness of 0.4 mm, while the PTFE thick sheath have a thickness of 1 mm. Therefore by comparing the experimental results of Nylon and PTFE thin sheaths, the effect of sheath material can be understood; and by comparing the results of PTFE thin and thick sheaths, we can determine the effect of sheath thickness.

Based on the number of types of cables and sheaths, there are twelve different combinations in total. And for each combination, we carry out experiments with two different bending angles, two different pretensions, two different cable speeds and two different sheath routing conditions. This results in a total of 144 different cases. In order to determine the variability and

reliability of the data, we performed five trials for each case and the averages and standard deviations of the force transmission efficiencies or elongation compliances introduced in the next section were calculated.

3.2 Evaluation Criteria

In this paper, we use force transmission efficiency defined by (3.1) and elongation compliance defined by (3.2) as the criteria to compare the experimental results of different cases. The force transmission efficiency is equal to the quotient of the change of the tension in the cable after the sheath, ΔT_{out} divided by that before the sheath, ΔT_{in}. And the elongation compliance is equal to the quotient of the cable elongation, δ divided by the change of the tension in the cable before the sheath, T_{in}. The force transmission efficiency represents the friction performance of a Bowden cable, and the elongation compliance represents the elongation performance. High force transmission efficiency and low elongation compliance is desired in a Bowden cable system.

$$E = \Delta T_{out}/\Delta T_{in} \tag{3.1}$$

$$C = \delta/\Delta T_{in} \tag{3.2}$$

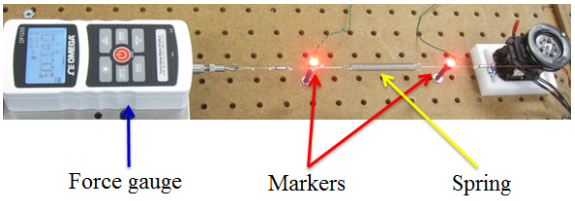

(a) Mechanical setup for validation

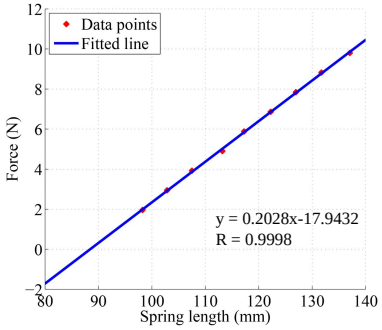

(b) Spring calibration result

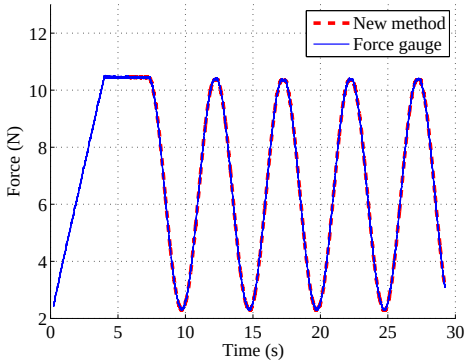

(c) Force data comparison

Figure 3.3: **Validation of the new force measurement method.** (a) The servo motor (Dynamixel RX-24F, ROBOTIS. Inc.) provides a sinusoidal force, which is measured both by using a digital force gauge (DFG55, OMEGA. Inc.) and the novel measurement method. (b) The force measurement system is calibrated using a set of weights. The fitted line has a correlation coefficient of 0.9998 which shows the spring has linear behavior. (c) The forces measured by the novel method and the force gauge are compared, the average error between the two sets of data is 0.01 N.

3.3 Measurement Method

3.3.1 Tension Measurement

To calculate the force transmission efficiency, we need to measure the input and output tension, T_{in} and T_{out}. Due to the large sensor weight or inertia compared with that of the cable, the common way of measuring tension using a load cell or force gauge may change the dynamic characteristics of the Bowden cable system and in turn affect the tension measurement accuracy. Thus instead of using a force sensor, we propose a novel tension measurement method using a motion capture system (PhaseSpace Inc.) and springs.

The idea is to attach markers to two ends of a spring, and insert the spring at any point where force is to be measured as shown in Fig. 3.3(a). Eight cameras are placed around the markers to capture the 3D motion of each marker. The deflection of the spring is recorded by the motion capture system, then the force is calculated using spring constant. Since the mass of a spring is fairly small, it has little effect on the dynamics of the original system.

To validate the performance of the novel tension measurement system, we first calibrated the spring and the experimental results show that the chosen spring has linear behaviour (Fig. 3.3(b)). Then we connected a motor, a string with the calibrated spring in series with a force gauge (Fig. 3.3(a)). We applied a sinusoidal force with the motor and measured it with both methods. The sampling rate of the force gauge is at 1000 Hz, while the novel measurement system runs at 480 Hz. Results show that the novel force measurement method is accurate in a dynamic setting. The two curves in Fig. 3.3(c) are almost the

same except for some data noises and the average error between the data from these two methods is around 0.01 N.

3.3.2 Elongation Measurement

The elongation of a Bowden cable means the change in cable length, which is determined by the relative positions of its two ends. Since the motion capture system records the real-time positions of the markers, the cable length as well as cable elongation, can be determined by attaching the markers to the cable ends. To simplify the measurement setup, we only measure the displacement of the motion capture marker attached to the input side of the cable while the output side of the cable is connected to a force gauge (DFG55, OMEGA. Inc.) fixed to the mechanical setup. The resolution of our elongation measurement method is 0.1 mm, which is determined by the resolution of the motion capture system.

3.4 Experimental Setup

Fig. 3.4 shows the experimental setups for friction and compliance characterization. The servo motor (Dynamixel RX-24F, ROBOTIS. Inc.) is used to load and unload the Bowden cable, the spring and marker sets are used to measure either the tension or the elongation of the cable, the clamps are used to hold the sheath, the pulleys are used for sheath routing, the force gauge is used to measure the pretension at the output side of the Bowden cable, and eight motion capture cameras (PhaseSpace Inc.) running at 480 Hz are placed

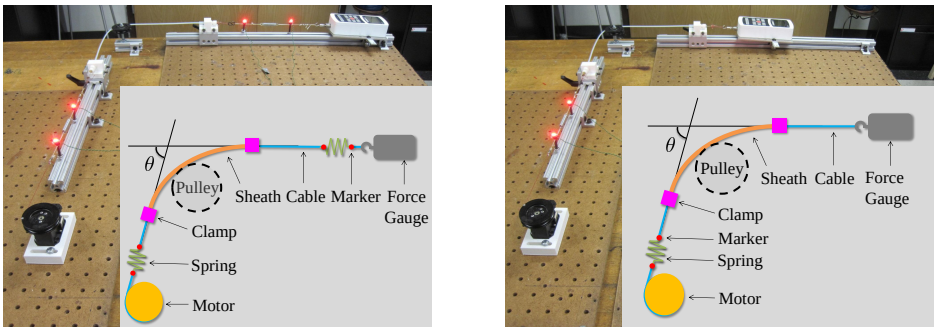

(a) Mechanical setup for friction characterization

(b) Mechanical setup for compliance characterization

Figure 3.4: **Experimental setup for** (a) friction characterization. Two springs attached with markers are used to measure the tension before and after the sheath. (b) compliance characterization. The spring attached to the input side of the cable is used to measure the cable elongation. θ is the clamp orientation.

around the markers to capture the 3D motion of each marker. Unlike the setup for friction characterization (Fig. 3.4(a)), there is no spring and marker set at the output side of the Bowden cable for the compliance characterization setup (Fig. 3.4(b)) because we only need the displacement of the marker attached to the input side of cable to determine the cable elongation.

3.5 Experiment Procedure

For each case, the experiment procedures are as follows: the motor loads the cable until the output tension measured by the force gauge reaches the required pretension 4 N. Next the motor loads and unloads the cable at 0.0153 m/s and this is repeated for the other cable speed 0.046 m/s with the

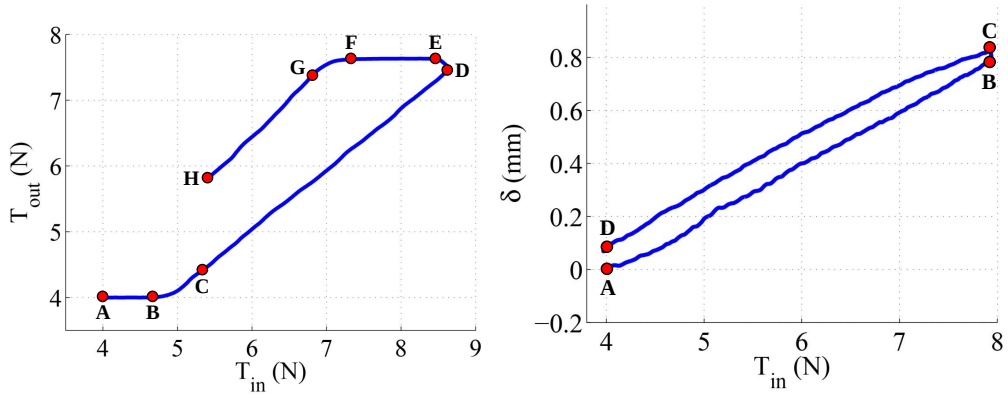

(a) Plot for friction characterization

(b) Plot for compliance characterization

Figure 3.5: **Typical plots of experiment trials** (a) A typical plot of one friction characterization experiment trial (1x7 stainless steel cable, PTFE thin sheath, 45° bending angle, 4 N pretension, 0.046 m/s cable speed, with routing pulley). A-E is the loading stage, while E-H is the unloading stage; (b) A typical plot of one compliance characterization experiment trial (FEP-coated small-diameter cable, PTFE thin sheath, 45° bending angle, 4 N pretension, 0.046 m/s cable speed, with routing pulley). A-B is the loading stage, B-C is the transition stage and C-D is the unloading stage

same pretension. Then the motor pretensions the cable to 6 N and loads and unloads the cable at 0.046 m/s. This completes one trial of a case. Then the collected data are processed as follows:

3.5.1 For Friction Characterization Experiments

The tensions in the cables are calculated and the output force T_{out} is plotted versus the input force T_{in}. Fig. 3.5(a)shows a representative plot for one experiment trial. The curve can be divided into 5 segments and they correspond to:

A-B the initial loading stage of the cycle. The coordinates of point A represent the pretensions in the cables before and after the sheath. From point A to B, T_{in} increases but T_{out} remains the same, meaning the input force has not been transmitted to the output side of the cable, and only partial of the cable is moving while the cable segment at the output side has not started moving yet.

B-C the loading transition stage. T_{in} is transmitted to the output T_{out} and the whole cable starts moving. Because it takes some time for the cable to reach the predetermined constant speed from zero, the transition segment has some curvature.

C-D the loading stage. The slope of this segment is equal to the loading force transmission efficiency.

D-E This segment corresponds to the loading to unloading transition stage. Because the motor stops much faster than the cable, the cable is still moving forward with a decreasing speed and T_{out} increases while T_{in} decreases till the cable stops moving.

E-H These segments are the unloading stages and match with the corresponding loading stages stated previously. The only difference is the direction of friction and cable movement is changed.

3.5.2 For Compliance Characterization Experiments

The cable elongation and the input tension are calculated, and the elongation δ is plotted versus the input force T_{in}. Fig. 3.5(b) shows a representative plot for one of the experiment trials. The curve can be divided into 3 segments: A-B is the loading stage of one cycle. The slope of this segment is equal to the loading elongation compliance; B-C is the transition stage from loading to unloading; and C-D is the unloading stage. The slope of this segment is equal to the unloading elongation compliance.

We only calculate the force transmission efficiency and elongation compliance for the loading stages because the data of the unloading stages usually fluctuate a lot.

Chapter 4

Experimental Results

In this section, the experimental results from both friction and compliance characterization are presented and the effects of various factors are discussed. Due to the large number of data, we only show the representative results. The presented results are consistent with the complete data set, which can be found in appendix.

4.1 Friction Characterization

4.1.1 Cable Construction (Fig. 4.1)

When the sheath is routed around a pulley, there is no significant difference in the force transmission efficiency between different cable constructions because the routing pulley reduces the difference in cable bending stiffness. However, if there is no pulley, the cable construction having larger bending stiffness leads to higher force transmission efficiency. This is because the cable runs through and supports the sheath. Large cable bending stiffness prevents the sheath from bending or buckling and reduces the total bending angles along the sheath. And according to the results in Bending Angle section, this helps to increase the efficiency.

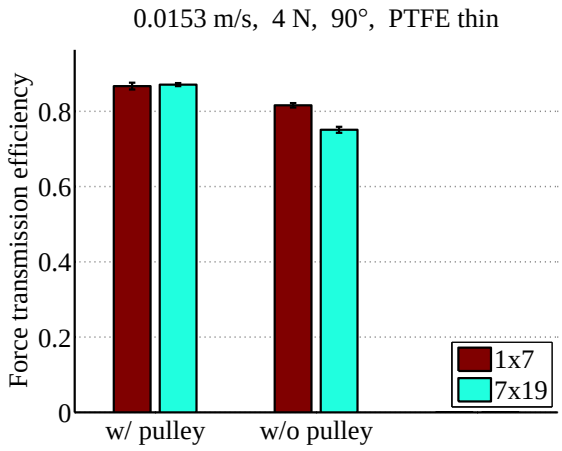

Figure 4.1: **Effects of cable construction on force transmission efficiency (PTFE thin sheath,** $90°$ **bending angle,** $4N$ **pretension,** $0.0153\ m/s$ **cable speed).** There is no significant difference in force transmission efficiency between different cable constructions, if the sheath is routed around a pulley. But cable construction (1x7) having larger bending stiffness leads to higher efficiency when there is no pulley.

4.1.2 Cable Diameter (Fig. 4.2)

When the sheath is routed around a pulley, there is no significant difference in the force transmission efficiency between different cable diameters because the routing pulley reduces the difference in cable bending stiffness. However, if there is no pulley, larger cable diameter leads to higher force transmission efficiency. This is because large cable diameter results in large cable bending stiffness, which in turn leads to high efficiency, as stated previously.

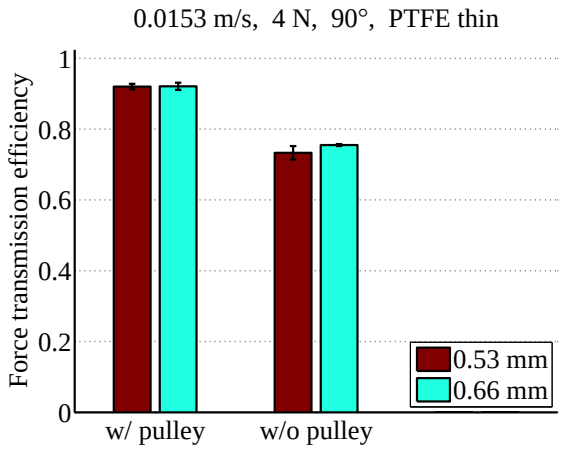

Figure 4.2: **Effects of cable diameter on force transmission efficiency (PTFE thin sheath, $90°$ bending angle, $4N$ pretension, 0.153 m/s cable speed).** There is no significant difference in force transmission efficiency between different cable diameters, if the sheath is routed around a pulley. But larger cable diameter ($0.66mm$) leads to slightly higher efficiency when there is no pulley.

4.1.3 Sheath Thickness (Fig. 4.3)

If there is no pulley, larger sheath thickness leads to much higher force transmission efficiency. This is because large sheath thickness results in large bending stiffness and high efficiency. When the sheath is routed around a pulley, the thicker sheath has slightly higher force transmission efficiency because the routing pulley reduces the difference in sheath bending stiffness.

4.1.4 Cable (Fig. 4.4) and Sheath Material (Fig. 4.5)

Smaller coefficient of friction of cable and sheath pair leads to higher force transmission efficiency for both cases with and without routing pulley. As

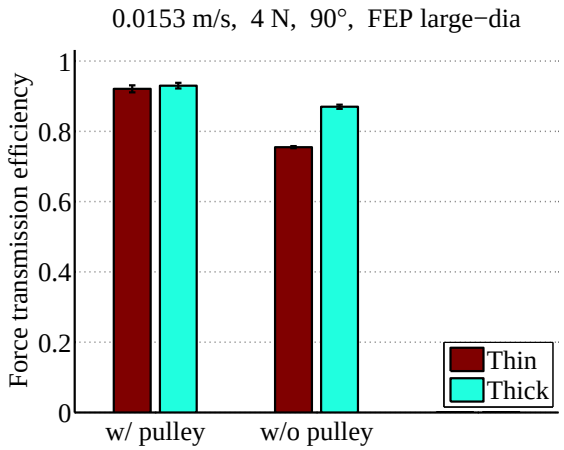

Figure 4.3: **Effects of sheath thickness on force transmission efficiency (7x19 FEP-coated large-diameter cable,** $90°$ **bending angle,** $4N$ **pre-tension,** 0.0153 m/s **cable speed).** Larger sheath thickness ($1mm$) leads to slightly higher force transmission efficiency when the sheath is routed around a pulley. If there is no pulley, the thicker sheath leads to much higher efficiency than the thinner one.

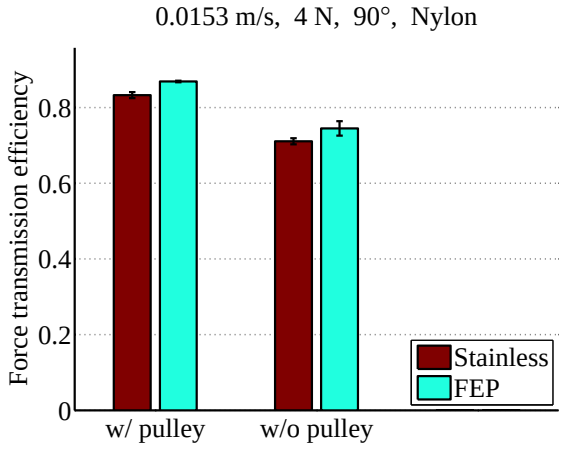

Figure 4.4: **Effects of cable material on force transmission efficiency (Nylon sheath, $90°$ bending angle, $4N$ pretension, 0.0153 m/s cable speed).** Pairing with the same sheath, the cable (7x19 FEP-coated large diameter stainless steel cable) having smaller coefficient of friction leads to higher efficiency for both cases with and without routing pulley.

Table 4.1: **Coefficient of friction of different cable and sheath pairs. The data is from the suppliers website (McMaster.com).**

		Cable	
		Stainless Steel	**FEP**
Sheath	**Nylon**	0.35	0.2
	PTFE	0.04	0.04

shown in Table 4.1, in terms of cable material, FEP has smaller coefficient of friction than stainless steel when paired with Nylon sheath. On the other hand, for sheath materials, PTFE has smaller coefficients of friction than Nylon when paired with stainless steel cable.

According to Table 4.1, stainless steel and FEP cables have the same

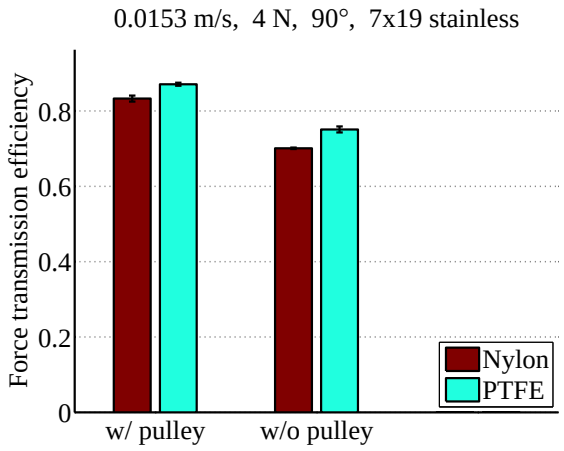

Figure 4.5: **Effects of sheath material on force transmission efficiency (7x19 stainless steel cable,** $90°$ **bending angle,** $4N$ **pretension,** $0.0153\ m/s$ **cable speed).** Pairing with the same cable, the sheath (PTFE thin sheath) having smaller coefficient of friction leads to higher efficiency for both cases with and without routing pulley.

coefficient of friction when paired with PTFE sheath. However, Fig. 4.6 shows that FEP cable has higher force transmission efficiency than stainless steel cable. The possible reason for this is that the coefficient of friction given in Table 4.1 is under the premise that both materials have the same surface roughness. However since the stainless steel cable is braided with multiple strands, its surface is relatively more rugged than that of the FEP-coated cable, which results in lower efficiency.

4.1.5 Bending Angle (Fig. 4.7)

Smaller bending angle leads to higher force transmission efficiency for both cases with and without routing pulley. This is because smaller bending angle

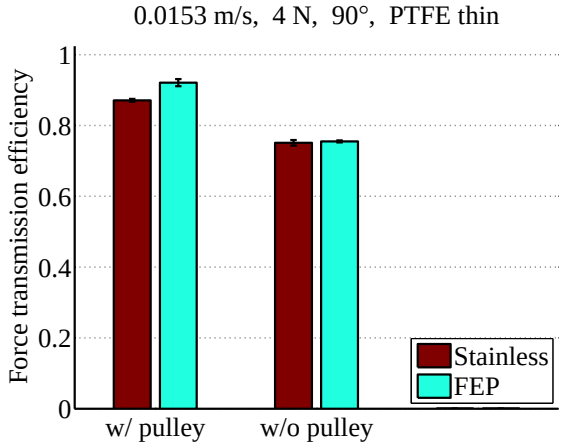

Figure 4.6: **Effects of cable material on force transmission efficiency (PTFE thin sheath, 90° bending angle, $4N$ pretension, 0.0153 m/s cable speed).** Although FEP and stainless steel cables have the same coefficient of friction when paired with PTFE sheath, FEP cable has shows higher force transmission efficiency than stainless steel cable.

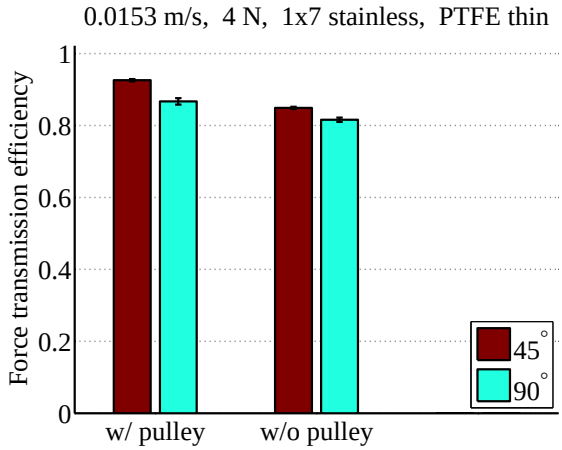

Figure 4.7: **Effects of bending angle on force transmission efficiency (PTFE thin sheath, 1x7 stainless steel cable, $4N$ pretension, 0.0153 m/s cable speed).** Smaller bending angle leads to higher force transmission efficiency for both cases with and without routing pulley.

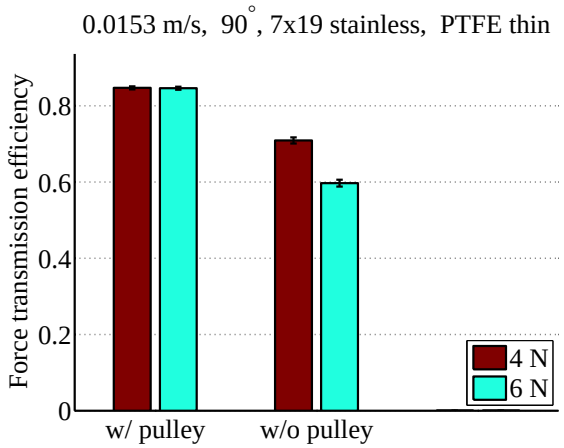

Figure 4.8: **Effects of pretension on force transmission efficiency (PTFE thin sheath, 90° bending angle, 7x19 stainless steel cable, 0.0153 m/s cable speed).** Pretension has no effect on force transmission efficiency when the sheath is routed around a pulley. But larger pretension leads to lower force transmission efficiency if there is no pulley.

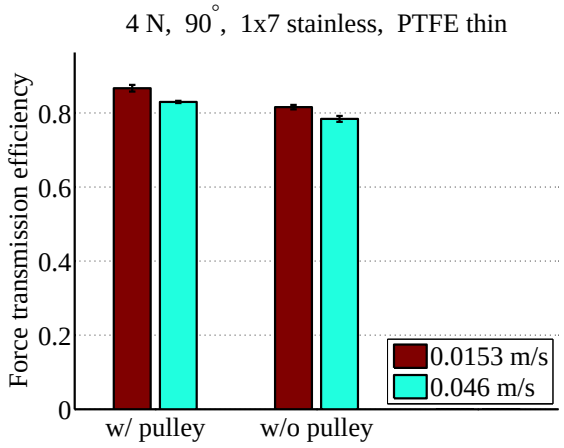

Figure 4.9: **Effects of speed on force transmission efficiency (PTFE thin sheath, 90° bending angle, $4N$ pretension, 1x7 stainless steel cable).** Larger cable speed leads to lower force transmission efficiency for both cases with and without pulley.

results in smaller normal force and friction force, and in turn increase the force transmission efficiency.

4.1.6 Pretension (Fig. 4.8)

Pretension has no effect on force transmission efficiency when the sheath is routed around a pulley. However, larger pretension leads to lower force transmission efficiency if there is no pulley. This is because when there is no routing pulley, larger pretension increases the total bending angle along the sheath and reduces the efficiency. But when the sheath is routed, the total bending angle remain the same, hence the efficiency does not change with pretension.

4.1.7 Cable Speed (Fig. 4.9)

Larger cable speed leads to lower force transmission efficiency for both cases with and without pulley. One reason for this is that Bowden cable friction includes some viscous friction. Another reason is that the coefficients of friction of the materials may increase with velocity.

4.1.8 Sheath Routing (Fig. 4.1–4.9)

We can see that for all different combinations of other factors, the cases with routing pulley always have higher force transmission efficiency than those without pulley. And the factors leading to the increase of bending stiffness of cables or sheaths help to reduce the difference in efficiency between cases with

and without routing pulley, because the major difference between cases with and without pulley is the bending stiffness.

4.2 Compliance Characterization

4.2.1 Cable Construction (Fig. 4.10)

Cable construction having larger elongation stiffness leads to smaller elongation compliance for both cases with and without pulley.

4.2.2 Cable Diameter (Fig. 4.11)

Larger cable diameter (0.66 mm) leads to lower compliance for both cases with and without routing pulley. This is because larger cable diameter results

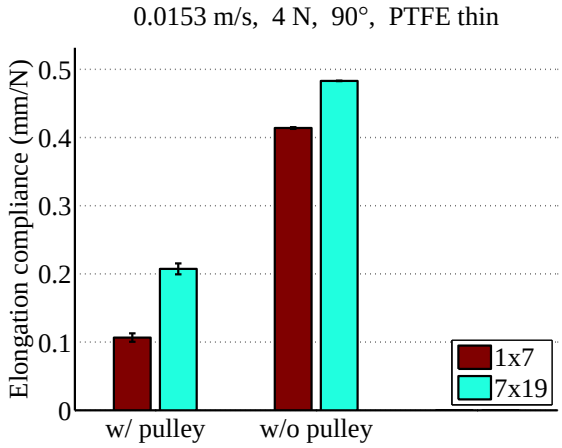

Figure 4.10: **Effects of cable construction on elongation compliance (PTFE thin sheath, 90° bending angle, $4N$ pretension, 0.0153 m/s cable speed).** Cable construction (1x7) having larger elongation stiffness leads to lower compliance for both cases with and without routing pulley.

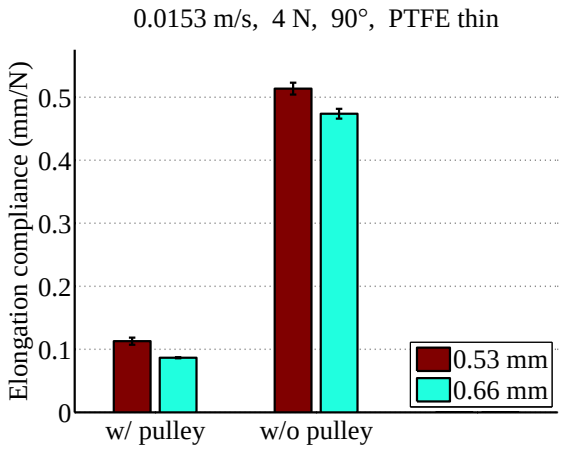

Figure 4.11: **Effects of cable diameter on elongation compliance (PTFE thin sheath,** $90°$ **bending angle,** $4N$ **pretension,** $0.0153\ m/s$ **cable speed).** Larger cable diameter ($0.66mm$) leads to lower compliance for both cases with and without routing pulley.

in larger cross section area and increase the elongation stiffness.

4.2.3 Sheath Thickness (Fig. 4.12)

When the sheath is routed around a pulley, thicker sheath leads to larger compliance. This is because the force along the cable is larger for the thicker sheath than the thinner sheath (Fig. 4.13), which causes the cable to be stretched more. If there is no routing pulley, larger sheath thickness leads to much smaller elongation compliance. This is because the elongation of cable is the combined result of the stretch of the cable and the shrink of the sheath. Smaller sheath thickness leads to smaller sheath elongation stiffness and the sheath shrinks more under given tension. Although the thicker sheath has higher force transmission efficiency and should have larger compliance as

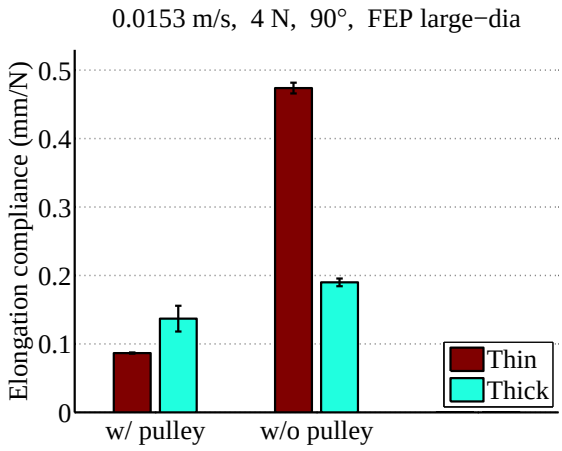

Figure 4.12: **Effects of sheath thickness on elongation compliance (7x19 FEP-coated large-diameter cable,** $90°$ **bending angle,** $4N$ **pre-tension,** $0.0153\ m/s$ **cable speed).** Larger sheath thickness ($1mm$) leads to larger compliance when the sheath is routed around a pulley, but it leads to much smaller compliance when there is no pulley.

the case with routing pulley, the shrink of sheath dominates the elongation compliance and the net result is that thinner sheath has larger compliance.

4.2.4 Cable and Sheath Material

We can not determine the effect of cable and sheath material on elongation compliance because the two cables and two sheaths not only have different material but different elongation stiffness as well. Therefore we can not tell the compliance difference is due to different material or it is due to different elongation stiffness.

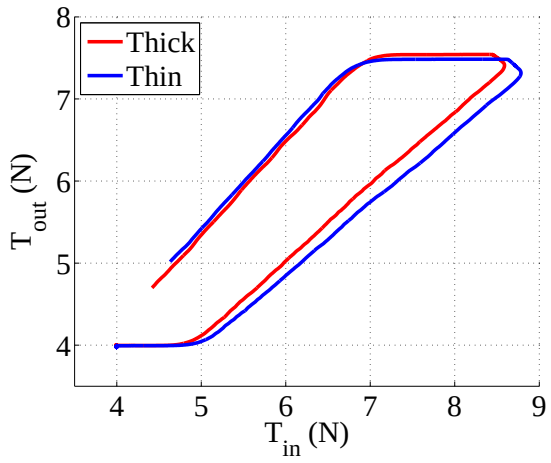

Figure 4.13: **Effects of sheath thickness on force transmission efficiency (7x19 FEP-coated large-diameter cable,** $90°$ **bending angle,** $4N$ **pretension,** $0.0153\ m/s$ **cable speed, with pulley).** Larger sheath thickness leads to higher force transmission efficiency and its output force is always larger than that of the thinner sheath during the loading phase.

4.2.5 Bending Angle (Fig. 4.14)

Smaller bending angle leads to larger elongation compliance. This is because smaller bending angle results in larger force transmission efficiency and larger force, and in turn increase the elongation compliance, as stated in Sheath Thickness section. .

4.2.6 Pretension (Fig. 4.15)

Pretension has no effect on elongation compliance for both cases with and without routing pulley. This is because pretension only affects the initial stretch of the cable. And the elongation compliance is calculated based on the

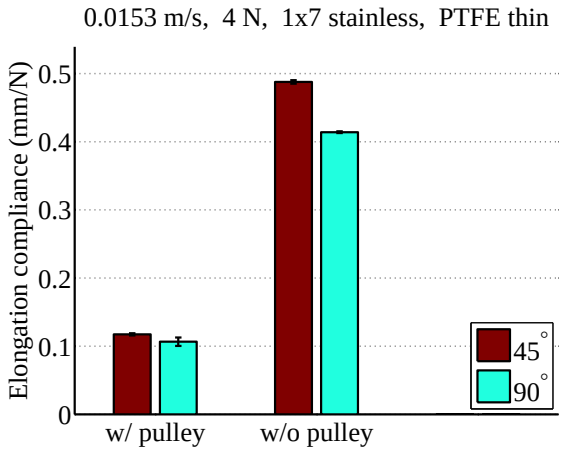

Figure 4.14: **Effects of bending angle on force transmission efficiency (PTFE thin sheath, 1x7 stainless steel cable,** $4N$ **pretension,** $0.0153\ m/s$ **cable speed).** Smaller bending angle leads to larger elongation compliance for both cases with and without routing pulley.

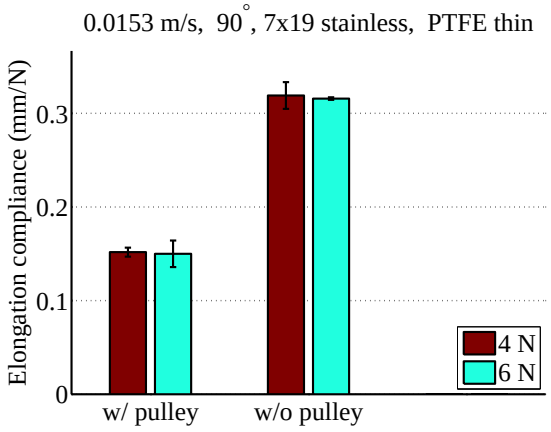

Figure 4.15: **Effects of pretension on force transmission efficiency (PTFE thin sheath,** $90°$ **bending angle, 7x19 stainless steel cable,** $0.0153\ m/s$ **cable speed).** Pretension has no effect on elongation compliance for both cases with and without routing pulley.

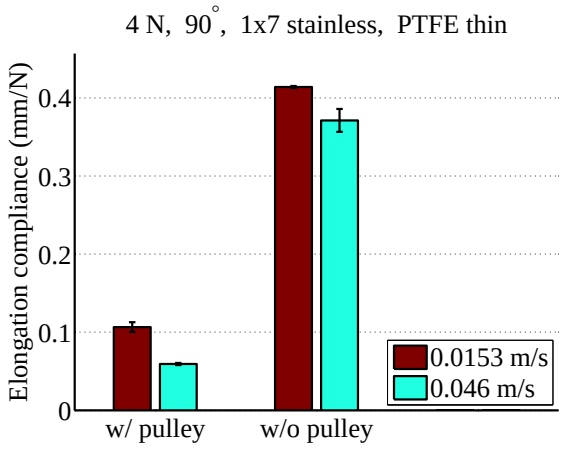

Figure 4.16: **Effects of speed on force transmission efficiency (PTFE thin sheath, 90° bending angle, 4N pretension, 1x7 stainless steel cable).** Larger cable speed leads to lower elongation compliance for both cases with and without pulley.

change of elongation and input force, not the absolute value of elongation and input force.

4.2.7 Cable Speed (Fig. 4.16)

Larger cable speed leads to smaller elongation compliance for both cases with and without pulley. This is because smaller cable speed results in larger force transmission efficiency and larger force, and in turn increase the elongation compliance, as stated in Sheath Thickness section.

4.2.8 Sheath Routing (Fig. 4.10–4.16)

We can see that for all different combinations of other factors, the cases with routing pulley always have smaller elongation compliance than those with-

out pulley. The routing pulley prevents the sheath from moving or buckling, which reduces the shrink of the sheath and results in smaller elongation compliance.

Chapter 5

Conclusions

We have presented a systematic experimental method for the characterization of Bowden cable friction and compliance.

We have investigated the effects of nine variables, including cable construction, cable diameter, cable material, sheath thickness, sheath material, bending angle, pretension, cable speed and sheath routing on force transmission efficiency and elongation compliance. In summary, cable construction having larger bending stiffness, larger cable diameter, larger sheath thickness, cable and sheath materials having smaller coefficient of friction, smaller bending angle, smaller cable speed and having the sheath routed around a pulley, result in increased force transmission efficiency. On the other hand, cable construction having larger elongation stiffness, larger cable diameter, larger sheath thickness (without routing pulley), smaller bending angle, larger cable speed and having the sheath routed around a pulley results in decreased elongation compliance.

We have introduced a novel force and elongation measurement method, and have validated its performance. By using the same system setup based on a motion capture system and springs, we can achieve both the measurement

of tension and cable elongation. And this helps to simplify our experimental setup.

Through a comprehensive set of experiments under 144 different situations, the following guidelines are generated. Robotics researchers could benefit from these results when choosing Bowden cables and designing control systems.:

Cable Construction Cable construction having larger bending stiffness helps to increase the force transmission efficiency and cable construction having larger elongation stiffness helps to decrease the elongation compliance.

Cable Diameter Larger cable diameter helps to increase the force transmission efficiency and decrease the elongation compliance.

Sheath Thickness Larger sheath thickness helps to increase the force transmission efficiency and decrease the elongation compliance.

Cable and Sheath Material Cable and sheath materials having smaller coefficient of friction helps to increase the force transmission efficiency.

Bending Angle Smaller bending angle helps to increase the force transmission efficiency, but increase the elongation compliance.

Cable Speed Smaller cable speed helps to increase the force transmission efficiency, but increase the elongation compliance.

Pretension Pretension has no effect on force transmission efficiency when the sheath is routed, but larger pretension decreases efficiency when there is no routing pulley. On the other hand, pretension has no effect on elongation compliance for both cases with and without routing pulley.

Sheath Routing Sheath routing has great effect on both force transmission efficiency and elongation compliance. Therefore, the previous studies [10, 11, 15, 17] based on routing pulleys may not be able to show the actual behavior of Bowden cables when the sheath is not routed. Generally, having the sheath routed around pulleys helps to increase the force transmission efficiency and decrease the elongation compliance.

One of the limitations of the study is that there may be potential correlations among the nine factors which was not investigated. Also this paper only studies the characteristics of small-sized Bowden cables, which are often used in robotic hand applications [1][4]. For characterizing Bowden cable for heavy load requirements, such as upper or lower limb robots, additional experiments might be necessary.

Our study may help robotics researchers in design of hardware and controller. The selection of actuator size is an important design decision and the estimation of external disturbance influences controls greatly. We provide spe-

cific guidelines for the selection of Bowden cable types and configurations, and the range of friction and cable elongation for the given condition based on the experimental analysis.

Appendix

Appendix 1

Data

Table 1.1 and Table 1.2 show the force transmission efficiencies for different cases. And Table 1.3 and Table 1.4 show the elongation compliances for different cases.

Table 1.1: **Force transmission efficiencies with the sheath routed around a pulley.** (FEP S means FEP-coated small-diameter cable, while FEP L means FEP-coated large-diameter cable.)

W/ Pulley				
Nylon, 90°	**1x7**	**7x19**	**FEP S**	**FEP L**
0.0153 m/s, 4 N	0.820(0.007)	0.833(0.008)	0.866(0.007)	0.869(0.011)
0.046 m/s, 4 N	0.795(0.006)	0.821(0.012)	0.860(0.020)	0.857(0.012)
0.046 m/s, 6 N	0.791(0.009)	0.817(0.008)	0.851(0.014)	0.852(0.015)
Nylon, 45°	**1x7**	**7x19**	**FEP S**	**FEP L**
0.0153 m/s, 4 N	0.872(0.015)	0.897(0.006)	0.923(0.008)	0.923(0.008)
0.046 m/s, 4 N	0.849(0.012)	0.881(0.017)	0.904(0.011)	0.909(0.003)
0.046 m/s, 6 N	0.847(0.006)	0.881(0.004)	0.907(0.007)	0.906(0.007)
PTFE thin, 90°	**1x7**	**7x19**	**FEP S**	**FEP L**
0.0153 m/s, 4 N	0.867(0.009)	0.871(0.004)	0.920(0.008)	0.921(0.010)
0.046 m/s, 4 N	0.830(0.003)	0.847(0.004)	0.884(0.010)	0.885(0.007)
0.046 m/s, 6 N	0.827(0.010)	0.846(0.007)	0.888(0.011)	0.884(0.008)
PTFE thin, 45°	**1x7**	**7x19**	**FEP S**	**FEP L**
0.0153 m/s, 4 N	0.926(0.003)	0.922(0.006)	0.950(0.002)	0.952(0.003)
0.046 m/s, 4 N	0.905(0.012)	0.898(0.005)	0.934(0.002)	0.935(0.011)
0.046 m/s, 6 N	0.895(0.001)	0.902(0.009)	0.936(0.003)	0.939(0.003)
PTFE thick, 90°	**1x7**	**7x19**	**FEP S**	**FEP L**
0.0153 m/s, 4 N	0.907(0.002)	0.919(0.010)	0.930(0.004)	0.930(0.008)
0.046 m/s, 4 N	0.898(0.006)	0.873(0.008)	0.921(0.010)	0.920(0.009)
0.046 m/s, 6 N	0.896(0.007)	0.871(0.017)	0.919(0.008)	0.919(0.008)
PTFE thick, 45°	**1x7**	**7x19**	**FEP S**	**FEP L**
0.0153 m/s, 4 N	0.923(0.013)	0.927(0.003)	0.948(0.009)	0.948(0.006)
0.046 m/s, 4 N	0.905(0.002)	0.915(0.004)	0.930(0.004)	0.931(0.006)
0.046 m/s, 6 N	0.909(0.009)	0.910(0.005)	0.930(0.008)	0.931(0.005)

Table 1.2: **Force transmission efficiencies without the sheath routed around a pulley.**(FEP S means FEP-coated small-diameter cable, while FEP L means FEP-coated large-diameter cable.)

W/O Pulley				
Nylon, 90°	**1x7**	**7x19**	**FEP S**	**FEP L**
0.0153 m/s, 4 N	0.724(0.009)	0.701(0.002)	0.720(0.008)	0.745(0.019)
0.046 m/s, 4 N	0.649(0.004)	0.643(0.003)	0.707(0.002)	0.730(0.011)
0.046 m/s, 6 N	0.567(0.012)	0.527(0.005)	0.676(0.016)	0.700(0.000)
Nylon, 45°	**1x7**	**7x19**	**FEP S**	**FEP L**
0.0153 m/s, 4 N	0.809(0.003)	0.773(0.009)	0.762(0.011)	0.765(0.004)
0.046 m/s, 4 N	0.777(0.001)	0.748(0.009)	0.744(0.006)	0.758(0.009)
0.046 m/s, 6 N	0.731(0.018)	0.708(0.009)	0.668(0.009)	0.727(0.010)
PTFE thin, 90°	**1x7**	**7x19**	**FEP S**	**FEP L**
0.0153 m/s, 4 N	0.816(0.006)	0.751(0.008)	0.733(0.019)	0.755(0.003)
0.046 m/s, 4 N	0.784(0.008)	0.709(0.008)	0.710(0.011)	0.730(0.008)
0.046 m/s, 6 N	0.756(0.007)	0.597(0.009)	0.703(0.000)	0.727(0.002)
PTFE thin, 45°	**1x7**	**7x19**	**FEP S**	**FEP L**
0.0153 m/s, 4 N	0.849(0.003)	0.766(0.002)	0.764(0.007)	0.777(0.013)
0.046 m/s, 4 N	0.822(0.004)	0.737(0.005)	0.727(0.002)	0.739(0.008)
0.046 m/s, 6 N	0.820(0.008)	0.650(0.004)	0.726(0.009)	0.731(0.010)
PTFE thick, 90°	**1x7**	**7x19**	**FEP S**	**FEP L**
0.0153 m/s, 4 N	0.877(0.008)	0.818(0.011)	0.849(0.004)	0.870(0.006)
0.046 m/s, 4 N	0.840(0.003)	0.792(0.006)	0.834(0.008)	0.814(0.005)
0.046 m/s, 6 N	0.784(0.014)	0.785(0.013)	0.766(0.008)	0.793(0.016)
PTFE thick, 45°	**1x7**	**7x19**	**FEP S**	**FEP L**
0.0153 m/s, 4 N	0.909(0.004)	0.892(0.004)	0.899(0.006)	0.904(0.007)
0.046 m/s, 4 N	0.888(0.006)	0.886(0.009)	0.885(0.005)	0.890(0.006)
0.046 m/s, 6 N	0.886(0.003)	0.873(0.005)	0.849(0.017)	0.869(0.020)

Table 1.3: **Elongation compliances with the sheath routed around a pulley.** (FEP S means FEP-coated small-diameter cable, while FEP L means FEP-coated large-diameter cable.)

W/ Pulley				
Nylon, 90°	**1x7**	**7x19**	**FEP S**	**FEP L**
0.0153 m/s, 4 N	0.1020(0.0316)	0.1651(0.0013)	0.1210(0.0161)	0.1095(0.0070)
0.046 m/s, 4 N	0.0520(0.0050)	0.0946(0.0059)	0.0863(0.0007)	0.0598(0.0076)
0.046 m/s, 6 N	0.0533(0.0037)	0.0850(0.0018)	0.0875(0.0115)	0.0573(0.0178)
Nylon, 45°	**1x7**	**7x19**	**FEP S**	**FEP L**
0.0153 m/s, 4 N	0.1236(0.0086)	0.1757(0.0046)	0.1411(0.0127)	0.1294(0.0064)
0.046 m/s, 4 N	0.0898(0.0094)	0.1048(0.0028)	0.1151(0.0021)	0.1090(0.0030)
0.046 m/s, 6 N	0.0862(0.0059)	0.1116(0.0056)	0.1404(0.0042)	0.0993(0.0013)
PTFE thin, 90°	**1x7**	**7x19**	**FEP S**	**FEP L**
0.0153 m/s, 4 N	0.1066(0.0062)	0.2074(0.0080)	0.1129(0.0057)	0.0866(0.0009)
0.046 m/s, 4 N	0.0593(0.0014)	0.1518(0.0048)	0.0853(0.0002)	0.0771(0.0036)
0.046 m/s, 6 N	0.0548(0.0076)	0.1500(0.0142)	0.0877(0.0055)	0.0727(0.0017)
PTFE thin, 45°	**1x7**	**7x19**	**FEP S**	**FEP L**
0.0153 m/s, 4 N	0.1174(0.0016)	0.2253(0.0142)	0.1422(0.0061)	0.1294(0.0062)
0.046 m/s, 4 N	0.0771(0.0025)	0.1842(0.0058)	0.1100(0.0014)	0.0809(0.0003)
0.046 m/s, 6 N	0.0784(0.0007)	0.1845(0.0021)	0.1145(0.0073)	0.0828(0.0029)
PTFE thick, 90°	**1x7**	**7x19**	**FEP S**	**FEP L**
0.0153 m/s, 4 N	0.1094(0.0027)	0.1934(0.0115)	0.1536(0.0037)	0.1369(0.0188)
0.046 m/s, 4 N	0.0875(0.0018)	0.0961(0.0014)	0.0986(0.0042)	0.0932(0.0033)
0.046 m/s, 6 N	0.0881(0.0025)	0.0935(0.0056)	0.0964(0.0028)	0.0930(0.0054)
DW45	**1x7**	**7x19**	**FEP S**	**FEP L**
0.0153 m/s, 4 N	0.1285(0.0032)	0.2559(0.0203)	0.1615(0.0050)	0.1687(0.0006)
0.046 m/s, 4 N	0.0938(0.0020)	0.1599(0.0000)	0.1042(0.0006)	0.0982(0.0042)
0.046 m/s, 6 N	0.1007(0.0083)	0.1583(0.0133)	0.1020(0.0033)	0.0958(0.0028)

Table 1.4: **Elongation compliances without the sheath routed around a pulley.** (FEP S means FEP-coated small-diameter cable, while FEP L means FEP-coated large-diameter cable.)

W/O Pulley				
Nylon, 90°	**1x7**	**7x19**	**FEP S**	**FEP L**
0.0153 m/s, 4 N	0.2385(0.0113)	0.3207(0.0051)	0.3172(0.0074)	0.2780(0.0043)
0.046 m/s, 4 N	0.1378(0.0092)	0.1262(0.0039)	0.0648(0.0016)	0.0835(0.0068)
0.046 m/s, 6 N	0.2645(0.0132)	0.1538(0.0077)	0.2647(0.0027)	0.1337(0.0006)
Nylon, 45°	**1x7**	**7x19**	**FEP S**	**FEP L**
0.0153 m/s, 4 N	0.2579(0.0076)	0.3189(0.0006)	0.2838(0.0045)	0.1666(0.0038)
0.046 m/s, 4 N	0.1343(0.0052)	0.1646(0.0116)	0.0854(0.0050)	0.1234(0.0073)
0.046 m/s, 6 N	0.1826(0.0016)	0.1681(0.0050)	0.1161(0.0066)	0.2371(0.0023)
PTFE thin, 90°	**1x7**	**7x19**	**FEP S**	**FEP L**
0.0153 m/s, 4 N	0.4140(0.0013)	0.4831(0.0003)	0.5136(0.0094)	0.4738(0.0078)
0.046 m/s, 4 N	0.3712(0.0147)	0.3191(0.0143)	0.3954(0.0051)	0.2425(0.0046)
0.046 m/s, 6 N	0.3626(0.0086)	0.3158(0.0014)	0.3650(0.0007)	0.2662(0.0001)
PTFE thin, 45°	**1x7**	**7x19**	**FEP S**	**FEP L**
0.0153 m/s, 4 N	0.4877(0.0026)	0.5221(0.0157)	0.5565(0.0105)	0.4128(0.0074)
0.046 m/s, 4 N	0.4152(0.0031)	0.4144(0.0006)	0.3686(0.0066)	0.2746(0.0003)
0.046 m/s, 6 N	0.4146(0.0082)	0.4031(0.0059)	0.3488(0.0000)	0.2789(0.0059)
PTFE thick, 90°	**1x7**	**7x19**	**FEP S**	**FEP L**
0.0153 m/s, 4 N	0.1612(0.0030)	0.1943(0.0070)	0.2193(0.0099)	0.1899(0.0056)
0.046 m/s, 4 N	0.1063(0.0057)	0.1528(0.0050)	0.1780(0.0038)	0.1526(0.0011)
0.046 m/s, 6 N	0.1419(0.0053)	0.1612(0.0098)	0.1784(0.0010)	0.1403(0.0010)
PTFE thick, 45°	**1x7**	**7x19**	**FEP S**	**FEP L**
0.0153 m/s, 4 N	0.1809(0.0053)	0.2091(0.0073)	0.2251(0.0090)	0.2143(0.0013)
0.046 m/s, 4 N	0.1532(0.0033)	0.1603(0.0018)	0.1763(0.0048)	0.1664(0.0041)
0.046 m/s, 6 N	0.1512(0.0022)	0.1615(0.0007)	0.1975(0.0019)	0.1637(0.0057)

Bibliography

[1] P. Agarwal, J. Fox, Y. Yun, M. K. OMalley, and A. D. Deshpande. An index finger exoskeleton with series elastic actuation for rehabilitation: Design, control and performance characterization. *International Journal of Robotics Research*, 2014. (under review).

[2] V. Agrawal, W.J. Peine, and Bin Yao. Modeling of transmission characteristics across a cable-conduit system. *IEEE Transactions on Robotics*, 26(5):914–924, 2010.

[3] Marcus Braun. Surgical instrument with elastically movable instrument head, October 18 2012. US Patent 20,120,265,176.

[4] L.B. Bridgwater, C.A. Ihrke, M.A. Diftler, M.E. Abdallah, N.A. Radford, J. M. Rogers, S. Yayathi, R. S. Askew, and D.M. Linn. The robonaut 2 hand - designed to do work with tools. In *IEEE International Conference on Robotics and Automation (ICRA)*, pages 3425–3430, May 2012.

[5] Lawrence E Carlson, Bradley D Veatch, and Daniel D Frey. Efficiency of prosthetic cable and housing. *Journal of Prosthetics and Orthotics*, 7(3):96–99, 1995.

[6] D. Chen, Y. Yun, and A. D. Deshpande. Experimental characterization of bowden cable friction. In *IEEE International Conference on Robotics*

and Automation (ICRA), 2014.

[7] Low Soon Chiang, Phee Soo Jay, P. Valdastri, A. Menciassi, and P. Dario. Tendon sheath analysis for estimation of distal end force and elongation. In *IEEE/ASME International Conference on Advanced Intelligent Mechatronics*, pages 332–337, July 2009.

[8] A Goiriena, I Retolaza, A Cenitagoya, F Martinez, S Riano, and J Landaluze. Analysis of bowden cable transmission performance for orthosis applications. In *IEEE International Conference on Mechatronics*, pages 1–6, 2009.

[9] M. Kaneko, W. Paetsch, and H. Tolle. Input-dependent stability of joint torque control of tendon-driven robot hands. *IEEE Transactions on Industrial Electronics*, 39(2):96–104, Apr 1992.

[10] M. Kaneko, M. Wada, H. Maekawa, and K. Tanie. A new consideration on tendon-tension control system of robot hands. In *IEEE International Conference on Robotics and Automation (ICRA)*, pages 1028–1033 vol.2, Apr 1991.

[11] M. Kaneko, T. Yamashita, and K. Tanie. Basic considerations on transmission characteristics for tendon drive robots. In *Fifth International Conference on Advanced Robotics (ICAR)*, pages 827–832 vol.1, June 1991.

[12] Kyoungchul Kong and Joonbum Bae. Torque mode control of a bowden cable-driven assistive system. In *International Conference on Control, Automation and Systems*, pages 1017–1020, 2012.

[13] Pierre Letier, Andre Schiele, M Avraam, M Horodinca, and A Preumont. Bowden cable actuator for torque-feedback in haptic applications. In *Eurohaptics Conference*, 2006.

[14] Jiting Li, Ruoyin Zheng, Yuru Zhang, and Jianchu Yao. iHandRehab: An interactive hand exoskeleton for active and passive rehabilitation. In *IEEE International Conference on Rehabilitation Robotics (ICORR)*, pages 1–6, 2011.

[15] Chen Lin, Wang Xingsong, and Tian Fuxiang. Tendon-sheath actuated robots and transmission system. In *International Conference on Mechatronics and Automation (ICMA)*, pages 3173–3178, Aug 2009.

[16] Thomas B Moeslund and Erik Granum. A survey of computer vision-based human motion capture. *Computer Vision and Image Understanding*, 81(3):231–268, 2001.

[17] G. Palli and C. Melchiorri. Model and control of tendon-sheath transmission systems. In *IEEE International Conference on Robotics and Automation (ICRA)*, pages 988–993, May 2006.

[18] A. Schiele. Performance difference of bowden cable relocated and non-relocated master actuators in virtual environment applications. In *IEEE/RSJ*

International Conference on Intelligent Robots and Systems (IROS), pages 3507–3512, 2008.

[19] A. Schiele and G. Hirzinger. A new generation of ergonomic exoskeletons - the high-performance x-arm-2 for space robotics telepresence. In *IEEE/RSJ International Conference on Intelligent Robots and Systems (IROS)*, pages 2158–2165, Sept 2011.

[20] A. Schiele, P. Letier, R. van der Linde, and F. van der Helm. Bowden cable actuator for force-feedback exoskeletons. In *IEEE/RSJ International Conference on Intelligent Robots and Systems*, pages 3599–3604, 2006.

[21] Andre Schiele, Pierre Letier, Richard Van Der Linde, and Frans Van Der Helm. Bowden cable actuator for force-feedback exoskeletons. In *IEEE/RSJ International Conference on Intelligent Robots and Systems (IROS)*, pages 3599–3604, 2006.

[22] James S Sulzer, Ronald A Roiz, Michael A Peshkin, and James L Patton. A highly backdrivable, lightweight knee actuator for investigating gait in stroke. *IEEE Transactions on Robotics*, 25(3):539–548, 2009.

[23] H. Vallery, J. Veneman, E. van Asseldonk, R. Ekkelenkamp, M. Buss, and H. van Der Kooij. Compliant actuation of rehabilitation robots. *IEEE Robotics Automation Magazine*, 15(3):60–69, September 2008.

[24] Shuang Wang, Jiting Li, and Ruoyin Zheng. Active and passive control algorithm for an exoskeleton with bowden cable transmission for

hand rehabilitation. In *IEEE International Conference on Robotics and Biomimetics*, pages 75–79, 2010.

[25] Zheng Wang, Zhenglong Sun, and Soo Jay Phee. Modeling tendon-sheath mechanism with flexible configurations for robot control. *Robotica*, 31:1131–1142, 2013.

[26] Barry Weitzner, John Golden, Richard Rothstein, Anna Chen, Dan Bacon, Kim Dang, et al. Medical device control system, November 15 2011. US Patent 8,057,462.

[27] Qingcong Wu and Xingsong Wang. Design of a gravity balanced upper limb exoskeleton with bowden cable actuators. Number 1, pages 678–683, 2013.